

Forum

Photomagnetism in Clusters and Extended Molecule-Based Magnets

Anne Bleuzen,^{*,†} Valérie Marvaud,^{*,‡} Corine Mathoniere,^{*,§} Barbara Sieklucka,^{*,||}
and Michel Verdaguer^{*,‡}

Chimie Inorganique, Institut de Chimie Moléculaire et des Matériaux d'Orsay, CNRS Unit 8182, Université Paris-Sud, Bâtiment 420, 91405 Orsay, France, Institut Parisien de Chimie Moléculaire, CNRS-UMR 7201, Case 42, Université Pierre et Marie Curie, 4 Place Jussieu, 75252 Paris Cedex 05, France, CNRS-UPR 9048, Institut de Chimie de la Matière Condensée de Bordeaux, 87 Avenue du Docteur Albert Schweitzer, Université Bordeaux 1, 33608 Pessac, France, and Faculty of Chemistry, Jagiellonian University, ul. R. Ingardena 3, 30-060 Krakow, Poland

Received October 20, 2008

Photomagnetism in molecular systems is a new development in molecular magnetism. It traces back to 1982 and 1984 when a transient effect and then the light-induced excited-spin-state-trapping effect was discovered in spin-crossover complexes. The present contribution gives a definition of the phenomenon, a process that changes the magnetism of a (molecular) system after absorption of a photon. It is limited to the discussion of photomagnetism based on *metal–metal electron transfer* in clusters and extended molecule-based magnets. The paper is organized around the main pairs of spin bearers, which allowed us to evidence and to study the phenomenon: Cu–Mo, Co–Fe, and Co–W. For each metallic pair, we report and discuss the conditions of appearance of the effect and its characteristics, both in extended structures and in molecular units: structure, spectroscopy, magnetism, thermodynamics and kinetics, and applications. We conclude with some brief prospects. The field is in rapid expansion. We are convinced that the interaction of photons with magnetized matter, to provide original magnetic properties, will meet more and more interest in the future.

1. Introduction

1.1. Photomagnetism and Magneto-optics. Photomagnetism can be defined as the process that changes the magnetism of a system after absorption of a photon. If R is the initial molecule and P the final one, molecular photomagnetism can be schematized as



R (reactant) is the initial molecule and P the final one (product). M_R and M_P are magnetizations of the reactant (R)

* To whom correspondence should be addressed. E-mail: michel.verdaguer@upmc.fr.

[†] Université Paris-Sud, CNRS. E-mail: annebleuzen@icmo.u-psud.fr.

[‡] Université Pierre et Marie Curie, CNRS. E-mail: valerie.marvaud@upmc.fr.

[§] Institut de Chimie de la Matière Condensée de Bordeaux, CNRS. E-mail: mathon@icmcb-bordeaux.cnrs.fr.

^{||} Jagiellonian University. E-mail: barbara.sieklucka@uj.edu.pl.

and product (P), respectively. They are different.

The absorption of light by matter can also simply heat the system, changing its magnetic properties, from a ferromagnetic to a paramagnetic phase, for example. This kind of trivial, nonquantum, interaction is not discussed here. We do not tackle the interaction of (linearly polarized) light by magnetized matter (Faraday or Kerr effects). We focus on the transformation of matter by light (photomagnetism) and not on the inverse phenomenon, the transformation of light by matter (magneto-optics).

1.2. Interaction between Spin and Photon. It is remarkable that a photon can change the magnetic state of a system because there is a priori a negligible interaction between a photon and an electronic spin. In the electromagnetic wave, the interaction of an electron with the electric field is much more important than the one with the magnetic field, thanks to the electric dipolar operator. In this contribution, we neglect the operators implying the magnetic field of the

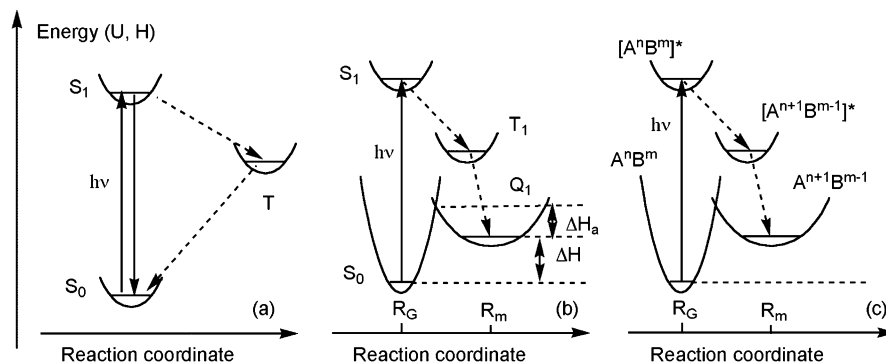


Figure 1. Potential energy scheme of ground and excited states of a molecular system after electronic transition versus an arbitrary reaction coordinate R (metal–ligand bond length, for example, in b) and c)...: (a) general three-state Jablonski diagram for a diamagnetic ground state with the ground-state singlet (S_0), the excited-state singlet (S_1), and the triplet T ; (b) in a LS Fe^{II} complex d^6 , (t_{2g})⁶, scheme of the formation of a trapped metastable state after an allowed transition to the excited-state singlet S_1 and two forbidden ICs to a triplet T_1 ($S = 1$) and to a quintet Q_1 ($S = 2$) (t_{2g})⁴(e_g)²; (c) simplified four-state potential energy diagram for a metal–metal charge transfer from the ground-state A^nB^m to the metastable $A^{n+1}B^{m-1}$. The solid arrows represent allowed transitions. The dotted arrows represent forbidden ICs.

electromagnetic wave. To be allowed, an electronic excitation must correspond to a constant spin process, $\Delta S = 0$ (S is the spin). If the ground-state wave function $|\varphi_G\sigma_G\rangle$, as well as the excited-state one $|\varphi_E\sigma_E\rangle$, is written as a spin orbital, the transition moment during the electronic excitation (with the electric dipolar operator O_{dip}) is

$$\mu \propto \langle \varphi_E\sigma_E | O_{\text{dip}} | \varphi_G\sigma_G \rangle \propto \langle \varphi_E | O_{\text{dip}} | \varphi_G \rangle \langle \sigma_E | \sigma_G \rangle$$

The dipolar electric operator acts only on the electronic, spatial, part (φ_G), not on the spin one (σ_G). The first factor in the expression at the right is often known as the Fermi golden rule. The second factor is controlled by the spin states. If we name α and β the up and down spin, respectively ($m_s = \pm 1/2$), the spin-allowed or spin-forbidden character of the transition appears simply when looking at the relations

$$\langle \alpha | \alpha \rangle = \langle \beta | \beta \rangle = 1 \quad \text{and} \quad \langle \alpha | \beta \rangle = \langle \beta | \alpha \rangle = 0$$

Indeed, in the well-known Jablonski diagram extensively used by photochemists, the first excitation for a diamagnetic material occurs from the ground-state singlet S_0 to an excited-state singlet S_1 in the so-called Franck–Condon conditions, without any geometrical and spin change (Figure 1a). Changes can come later with a forbidden intersystem crossing (IC) to a triplet (T). The radiative deexcitation from S_1 to S_0 (fluorescence, no change in spin) is allowed, but the T to S_0 deexcitation (phosphorescence, spin change) is forbidden. The transition being forbidden, the lifetime of the excited-state triplet T , is longer than the one of the excited-state singlet S_1 : the property is useful in luminescent applications but less easily handled in magnetic ones. The same spin selection rules hold when photon absorption is followed by electron transfer (see section 1.4).

Because spin changes under irradiation have been observed experimentally in the spin-crossover systems, with a significant lifetime of the resulting species, we first take a brief look at them.

1.3. Brief Look at the Photomagnetic Effect in Spin-Crossover Systems. The first observation of a photomagnetic process in a molecular spin-crossover system was made in a transient system by McGarvey and Lawthers in

1982^{1a} and then by Decurtins and co-workers in 1984.^{1b}

A spin crossover is the spin change of a transition-metal complex [from high spin (HS) to low spin (LS) or the contrary]. Spin crossover can occur under the influence of temperature, pressure, light, magnetic field, etc. In the thermal process, it is driven by variation of the free enthalpy $\Delta G = \Delta H - T\Delta S$ ($\Delta G = G_{\text{HS}} - G_{\text{LS}}$; $\Delta H = H_{\text{HS}} - H_{\text{LS}} > 0$; $\Delta S = S_{\text{HS}} - S_{\text{LS}} > 0$). At the temperature when $\Delta G = 0$, $T = \Delta H/\Delta S = T_{1/2}$, where the HS fraction x is $1/2$. When elastic interactions occur between the spin bearers, hysteresis and bistability can result. The phenomenon is well documented and gives rise to exciting new prospects in molecular magnetism.^{1–3}

The photoinduced process evidenced in 1984 in spin-crossover systems is named the light-induced excited-spin-

- (1) (a) McGarvey, J. J.; Lawthers, J. *J. Chem. Soc., Chem. Commun.* **1982**, 906. (b) Decurtins, S.; Gütllich, P.; Köhler, C. P.; Spiering, H.; Hauser, A. *Chem. Phys. Lett.* **1984**, 105, 1.
- (2) (a) Gütllich, P.; Hauser, A.; Spiering, H. *Angew. Chem.* **1994**, 33, 2024. (b) Gütllich, P.; Garcia, Y.; Woike, T. *Coord. Chem. Rev.* **2001**, 219, 839. (c) Sorai, M. *J. Chem. Thermodyn.* **2002**, 34, 1207. (d) Varret, F.; Noguès, M.; Goujon, A. In *Magnetism: Molecules to Materials*; Miller, J., Drillon, M., Eds.; Wiley: New York, 2001; Vol. 2, p 257. (e) Varret, F.; Bleuzen, A.; Boukhedaden, K.; Bousseksou, A.; Codjovi, E.; Enachescu, C.; Goujon, A.; Linares, J.; Menendez, N.; Verdaguer, M. *Pure Appl. Chem.* **2002**, 74, 2159. (f) Real, J. A.; Gaspar, A. B.; Muñoz, M. C. *Dalton Trans.* **2005**, 2062, 2079. (g) Gütllich, P.; Goodwin, H. A., Eds. *Spin Cross over in Transition Metal Compounds*; Springer: Berlin, 2004; Vols. I–III. (h) Bonhommeau, S.; Molnár, G.; Galet, A.; Zwick, A.; Real, J. A.; McGarvey, J. J.; Bousseksou, A. *Angew. Chem., Int. Ed.* **2005**, 44, 4069. (i) Cobo, S.; Ostrovskii, D.; Bonhommeau, S.; Vendier, L.; Molnár, G.; Salmon, L.; Tanaka, K.; Bousseksou, A. *J. Am. Chem. Soc.* **2008**, 130, 9019. (j) Molnár, G.; Cobo, S.; Real, J. A.; Carcenac, F.; Daran, E.; Vieu, C.; Bousseksou, A. *Adv. Mater.* **2007**, 19, 2163. (k) Duriska, M. B.; Neville, S. M.; Moubaraki, B.; Cashin, J. D.; Halder, G. J.; Chapman, K. W.; Balde, C.; Létard, J. F.; Murray, K. S.; Kepert, C. J.; Batten, S. R. *Angew. Chem., Int. Ed.* **2008**, 47, 1.
- (3) (a) Boillot, M.-L.; Roux, C.; Audière, J.-P.; Dausse, A.; Zarembowitch, *J. Inorg. Chem.* **1996**, 35, 3975. (b) Boillot, M.-L.; Chantraine, S.; Zarembowitch, J.; Lallemand, J. Y.; Prunet, J. J. *New J. Chem.* **1999**, 179.
- (4) (a) Pierpont, C. G. *Coord. Chem. Rev.* **2001**, 219, 99. (b) Hendrickson, D. N.; Pierpont, C. G. *Top. Curr. Chem.* **2004**, 234, 63. (c) Dei, A.; Gatteschi, D.; Sangregorio, C.; Sorace, L. *Acc. Chem. Res.* **2004**, 37, 827. (d) Evangelio, E.; Ruiz-Molina, D. *Eur. J. Inorg. Chem.* **2005**, 2957.
- (5) (a) Sato, O.; Iyoda, T.; Fujishima, A.; Hashimoto, K. *Science* **1996**, 272, 704. (b) Sato, O.; Einage, Y.; Iyoda, T.; Fujishima, A.; Hashimoto, K. *J. Electrochem. Soc.* **1997**, 144, 11. (c) Verdaguer, M. *Science* **1996**, 272, 698.

state-trapping (LIESST) effect because it corresponds to the trapping of an excited HS state thanks to the energy barrier between the excited state and the ground state impeding the system from going back to the ground state: it corresponds to the formation of a rather robust metastable state, first identified at low temperature.

The phenomenon has been thoroughly investigated. Useful reviews are available and can be found in a beautiful review article,^{2a} more recent reviews,^{2b-f} and a collective contribution.^{2g} A crude scheme of the potential energy of the main spin states of an Fe^{II} octahedral complex with six d electrons is shown in Figure 1b as a function of the reaction coordinate that is the distance R between the metal and ligand. The LS ground-state distance R_G is smaller than the HS metastable distance R_m . The LS state S_0 has a lower enthalpy H_{LS} than the quintet Q_1 HS state H_{HS} ($\Delta H = H_{HS} - H_{LS} > 0$). At low temperature, it exists an energy barrier ΔH_a between the excited quintet Q_1 and the ground singlet, hence able to *trap* the quintet as a *metastable* state. A triplet intermediate spin state T_1 is also shown.

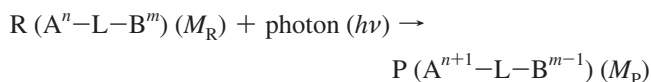
A clever variant of spin crossover consists of provoking the spin change by an electronic excitation on a photoisomerizable ligand. For example a cis–trans double-bond photoisomerization can vary the ligand field of the metal ion enough to achieve the spin crossover. This is named the ligand-driven light-induced spin crossover (LD-LISC).³ Its advantage is to present a robust, long-lifetime, metastable state on a wide range of temperatures. Both phenomena, LIESST and LD-LISC effects, have been observed at room temperature.^{2g-i,3b} New spin-crossover systems present wide hysteresis^{2g-i} and reversible quick switching²ⁱ from one state to the other around room temperature. Together with new studies about the behavior of nanosystems,^{2j,k} this opens new and bright perspectives.

1.4. Metal–Metal Charge-Transfer Systems and the Scope of the Article. We are dealing in this Article with a few examples of changes of the magnetization of the matter upon irradiation accompanied by an electron transfer from one metallic center to another. The case of photoinduced electron transfer implying a noninnocent ligand L (valence tautomerism equilibrium)⁴



where, for example, A is Co^{II}, L⁰ a semiquinone, and L⁻¹ is a catechol,^{4a,b} is not included in the present review.

We consider only cases where the initial compound (reactant) is a bimetallic system (A^n-L-B^m , L being a ligand, A^{n+} and B^{m+} different transition-metal ions in oxidation states n and m , A^nB^m). The irradiation forms an excited state $[A^nB^m]^*$, which is deexcited to the metastable state $A^{n+1}B^{m-1}$ in a series of steps including electron transfer and subsequent spin changes such as $[A^{n+1}B^{m-1}]^*$ (see Figure 1c):



The electron transfer and the spin change are associated with a different population of the d orbitals and especially of the antibonding e_g^* ones (when the metallic ion is octahedral). This leads to important geometrical changes around the transition metal. It is then possible to follow the process by using one of the metal–ligand distances (A–L) as the reaction coordinate R of the process (Figure 1c). The change in the geometry accompanying the change in the e_g^* orbital occupation is one of the keys of the creation of the energy barrier between the metastable and ground states. Indeed, Figure 1 shows examples of a generic potential energy diagram of two-state switchable molecular systems, behaving as harmonic oscillators, applicable to many cases: spin crossover,^{2,3} mixed valence (see Figure 14), electron transfer, valence tautomerism,⁴ etc.

The scope of the paper is limited to a few examples of metal-to-metal charge transfer with $A-L-B = A-NC-B = Co-NC-Fe$, $Cu-NC-Mo$, etc. For a given transition-metal pair AB, we present systems that can be polynuclear molecular complexes or networks of different dimensionalities: one-, two-, or three-dimensional (1D, 2D, or 3D). For molecules, the system remains paramagnetic after irradiation, but the spin is changed, forming, for example, photomagnetic HS molecules. For 3D networks, thanks to cooperative effects, irradiation can lead to spectacular changes in the long-range magnetic order (enhancement of magnetization in the magnetically ordered phase and of the Curie temperature). In both cases, we try to give a clear chemical and physical characterization of the systems and its up-to-date interpretation, even if a complete description of the different excited spin states is very complex. A discussion about the technical aspects and difficulties of measurements (sample heating, sample absorption impeding complete transformation, etc.) can be found in ref 2d.

2. Photoactivity of CoFe Prussian Blue Derivatives

2.1. Photoactive CoFe Prussian Blue Analogue Extended Network. The first photomagnetic effect in Prussian blue analogues was reported by Hashimoto and co-workers in 1996 in the analogue of chemical formula $K_{0.4}Co_{1.3}[Fe(CN)_6]_1 \cdot 5H_2O$.^{5a,b} The Japanese team showed that the magnetization and the magnetic ordering temperature of this compound increased under irradiation by visible light at low temperature. This discovery opened a new field of investigation. “Molecular electronics emerges in molecular magnetism” said a comment.^{5c} Indeed, the search for molecular systems exhibiting photomagnetic properties is expanding.

The photomagnetic properties of CoFe Prussian blue analogues were rapidly optimized, and photomagnetic analogues able to switch from a nearly diamagnetic state to a magnetically ordered one were synthesized.^{6,7} The magnetization of those photomagnetic CoFe Prussian blue analogues, very low before irradiation, strongly increases under

(6) Shimamoto, N.; Ohkoshi, S.-i.; Sato, O.; Hashimoto, K. *Inorg. Chem.*, **2002**, *41*, 678.

(7) Bleuzen, A.; Lomenech, C.; Escax, V.; Villain, F.; Varret, F.; Cartier dit Moulin, C.; Verdaguer, M. *J. Am. Chem. Soc.* **2000**, *122*, 6648.

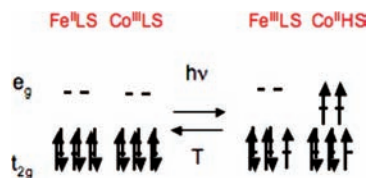


Figure 2. Oxidation and spin states of the transition-metal ions in a photoactive pair of CoFe Prussian blue analogues in the ground state (left) and in the photoinduced metastable state (right).

irradiation by visible light at low temperature. When the light is switched off, their magnetization remains very high. The compounds are trapped in a metastable state of long lifetime at low temperature. The metastable excited state behaves as a magnet below a Curie temperature of around 21 K. Through heating, the initial magnetization is recovered. The metastable state relaxes to the ground state, with relaxation temperatures ranging from about 90 to 150 K.^{6,8,9} The results demonstrate that such compounds can be used to write and store some information and that the information can be thermally erased. Nevertheless, before they can be used as useful rewritable photomagnetic memories, a crucial problem needs to be solved, the strong enhancement of the critical temperature.

Since the discovery of the phenomenon, it has been shown that light is not the only external strain able to trigger the switch of the compounds: the magnetization can be changed by varying the temperature, by varying the pressure,¹⁰ or by replacing the alkali cation inserted in the 3D structure.¹¹ The switch of one sodium derivative from one state to the other in a thermal hysteresis loop near room temperature by a one-shot laser pulse has also been reported.¹²

The electronic structure of the states implied in the switching properties of the CoFe Prussian blue analogues is now well-known. The ground state is composed of diamagnetic Co^{III}–LS Fe^{II} pairs, which are transformed into Co^{II}–HS Fe^{III} ones after irradiation. The photomagnetic effect is due to a photoinduced electron transfer accompanied by a spin change of the cobalt ion (Figure 2).¹³

In the metastable state, both transition-metal ions bear a magnetic moment. If the determination of the nature of the exchange interaction between paramagnetic ions is often trivial for compounds with known structure and chemical formula by an examination of the $\chi_M T$ and saturation

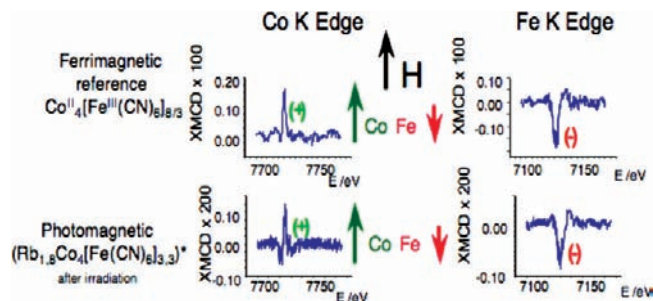


Figure 3. XMCD signals at the Co K edge in the alkali-cation-free ferrimagnetic reference at 10 K (left, top) and in the photomagnetic compound after irradiation at 10 K (left, bottom) and dichroic signals at the Fe K edge in the alkali-cation-free ferrimagnetic reference at 10 K (right, top) and in the photomagnetic compound after irradiation at 10 K (right, bottom).

magnetization curves, such macroscopic characterization proves impossible for the photoinduced state because (i) the irradiation of the sample is not necessarily complete and the mass of the transformed phase is therefore unknown and (ii) the thermal relaxation of the photoinduced state makes impossible any analysis of the $\chi_M T$ curve. X-ray magnetic circular dichroism (XMCD) allowed the determination of the relative orientations of the magnetic moment born by the two cations.¹⁴ The macroscopic magnetization data of the alkali-cation-free CoFe Prussian blue analogue are well-known and clearly show an antiferromagnetic coupling between the cobalt and iron ions. The macroscopic observation finds its local counterpart in the dichroic signals (Figure 3, top): at the Co K edge, the dichroic signal is positive, whereas it is negative at the Fe K edge. This inversion of the dichroic signal from cobalt to iron is a local characterization of the antiferromagnetic coupling between both ions. In the photoinduced state of the photomagnetic compound of chemical formula $\text{Rb}_{1.5}\text{Co}_4[\text{Fe}(\text{CN})_6]_{3.3} \cdot 13\text{H}_2\text{O}$ (Figure 3, bottom), the dichroic signal is also positive at the Co K edge and negative at the Fe K edge, which evidences the antiferromagnetically coupling in the photoinduced state.

The transformation of LS Co^{III} ions into HS Co^{II} ions with the population of antibonding orbitals is expected to be accompanied by an increase of the cobalt-to-ligand bonds. Such a photoinduced local structural change in the powdered samples has been detected by extended X-ray absorption fine structure (EXAFS) at the Co K edge (Figure 4).^{15,16}

The shift of the EXAFS signal toward lower k indicates a cobalt-to-ligand bond lengthening after irradiation. The simulation of the first peak of the Fourier transform modulus allowed the quantitative determination of the cobalt-to-ligand bonds in the ground and photoexcited states. The length of the cobalt-to-ligand bonds increases from 1.91 Å in the diamagnetic state (LS Co^{III}–LS Fe^{II}) up to 2.08 Å in the metastable excited state (HS Co^{II}–LS Fe^{III}). Such a local

- (8) (a) Gawali-Salunke, S.; Varret, F.; Maurin, I.; Enachescu, C.; Malarova, M.; Boukheddaden, K.; Codjovi, E.; Tokoro, H.; Ohkoshi, S.; Hashimoto, K. *J. Phys. Chem. B* **2005**, *109*, 8251. (b) Varret, F.; Boukheddaden, K.; Codjovi, E.; Maurin, I.; Tokoro, H.; Ohkoshi, S.; Hashimoto, K. *Polyhedron* **2005**, *24*, 2857.
- (9) Escax, V.; Bleuzen, A.; Cartier dit Moulin, C.; Villain, F.; Goujon, A.; Varret, F.; Verdager, M. *J. Am. Chem. Soc.* **2001**, *123*, 12536.
- (10) (a) Ksenofontov, V.; Levchenko, G.; Reiman, S.; Gütllich, P.; Bleuzen, A.; Escax, V.; Verdager, M. *Phys. Rev. B* **2003**, *68*, 024415. (b) Hanawa, H.; Moritomo, Y.; Tateishi, J.; Ohishi, Y.; Kato, K. *J. Phys. Soc. Jpn.* **2004**, *73*, 2750.
- (11) Sato, O.; Einaga, Y.; Iyoda, T.; Fujishima, A.; Hashimoto, K. *J. Phys. Chem. B* **1997**, *101*, 3903.
- (12) (a) Shimamoto, N.; Ohkoshi, S.; Sato, O.; Hashimoto, K. *Chem. Lett.* **2002**, *31*, 486. (b) Liu, H. W.; Matsuda, K.; Gu, Z. Z.; Takahashi, K.; Cui, A. L.; Nakajima, R.; Fujishima, A.; Sato, O. *Phys. Rev. Lett.* **2003**, *90*, 167403.
- (13) Cartier dit Moulin, C.; Villain, F.; Bleuzen, A.; Arrio, M.-A.; Sainctavit, P.; Lomenech, C.; Escax, V.; Baudelet, F.; Dartyge, E.; Gallet, J. J.; Verdager, M. *J. Am. Chem. Soc.* **2000**, *122*, 6653.

- (14) Champion, G.; Escax, V.; Cartier dit Moulin, C.; Bleuzen, A.; Villain, F.; Baudelet, F.; Dartyge, E.; Verdager, M. *J. Am. Chem. Soc.* **2001**, *123*, 12544.
- (15) (a) Yokoyama, T.; Ohta, T.; Sato, O.; Hashimoto, K. *Phys. Rev. B: Condens. Matter* **1998**, *58*, 8257. (b) Yokoyama, T.; Kiguchi, M.; Ohta, T.; Sato, O.; Einaga, Y.; Hashimoto, K. *Phys. Rev. B: Condens. Matter* **1999**, *60*, 9340.
- (16) Escax, V.; Bleuzen, A.; Itié, J.-P.; Münsch, P.; Varret, F.; Verdager, M. *J. Phys. Chem. B* **2003**, *107*, 4763.

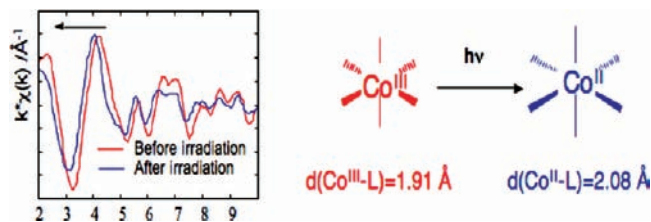


Figure 4. EXAFS signal at the Co K edge of the photomagnetic compound of chemical formula $\text{Rb}_2\text{Co}_4[\text{Fe}(\text{CN})_6]_{3.3} \cdot 13\text{H}_2\text{O}$ before and after irradiation at 10 K.

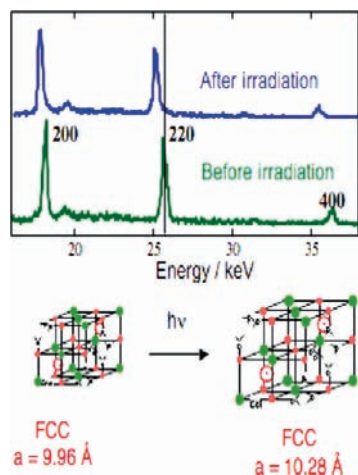


Figure 5. Energy-dispersive XRD pattern of the photomagnetic compound of chemical formula $\text{Rb}_2\text{Co}_4[\text{Fe}(\text{CN})_6]_{3.3} \cdot 13\text{H}_2\text{O}$ at 10 K before and after irradiation.

structural change is also necessarily accompanied by a long-range-order change, which has been studied by energy-dispersive XRD (Figure 5).¹⁷

The ground and metastable states exhibit the well-known face-centered-cubic structure of Prussian blue analogues,¹⁸ but the cell parameter is much longer after irradiation. The photomagnetic effect is accompanied by a significant increase of the cell parameter from 9.96 Å in a state essentially composed of diamagnetic (LS Co^{III} –LS Fe^{II}) pairs with short cobalt-to-ligand bonds to 10.28 Å in the photoexcited (HS Co^{II} –LS Fe^{III}) state with longer cobalt-to-ligand bonds.

The chemical formula of CoFe Prussian blue analogues is given by $\text{C}_x\text{Co}_4[\text{Fe}(\text{CN})_6]_{(8+x)/3} \cdot n\text{H}_2\text{O}$ where C^+ is an alkali-metal ion. Like all Prussian blue analogues, CoFe analogues are versatile compounds, the chemical composition of which can be infinitely varied: the nature of the alkali-metal ion, the amount of the alkali-metal ion from 0 to 4 per cell, which is linked to the amount of $[\text{Fe}(\text{CN})_6]$ vacancies, and the amount of water molecules. Any change of the chemical composition affects the photomagnetic properties of the compounds. Thus, compounds containing various amounts of the same alkali cation exhibit different magnetic and photomagnetic properties (Figure 6, top), and compounds exhibiting the same stoichiometry $\text{C}_2\text{Co}_4\text{[Fe}(\text{CN})_6]_{3.3} \cdot 13\text{H}_2\text{O}$, in which only the nature of the alkali varies, also show different magnetic and photomagnetic

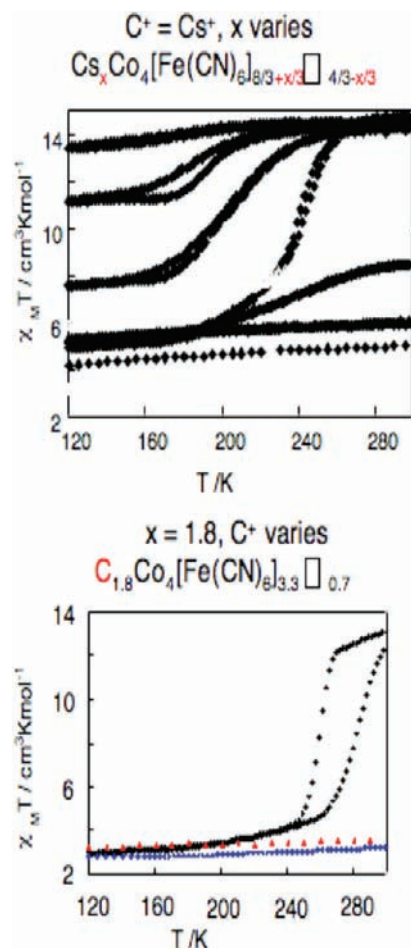


Figure 6. Magnetic properties of CoFe compounds of the chemical formula $\text{C}_x\text{Co}_4[\text{Fe}(\text{CN})_6]_{(8+x)/3} \cdot n\text{H}_2\text{O}$, where x is changing (above) [x varies from 0 at the top to 4 at the bottom], and $\text{C}_{1.8}\text{Co}_4[\text{Fe}(\text{CN})_6]_{3.3} \cdot 13\text{H}_2\text{O}$, where C is changing (below) [$\text{C} = \text{Na}$, black; Rb , red; Cs , blue].

properties (Figure 6, bottom). The thermal variation of the $\chi_M T$ product evidences a thermally activated electron transfer. The magnitude of the electron transfer and the temperature range over which it occurs strongly depend on the amount⁴ (Figure 5a) and the nature (Figure 5b) of the alkali cation in the structure.

If the electronic structure of the transition-metal ion in the ground and metastable states is now well-known, questions still remain on the atomic arrangement of the cyanide bridges, water molecules, and alkali cations,¹⁹ on the interactions between those species in the 3D structure, and on the role of the different species in the switching properties of the compounds. Also, possible differences between the thermally quenched and photoinduced states remain a question for future research.

2.2. Photoactive CoFe Prussian Blue Nanoparticles.

Photomagnetic CoFe Prussian blue analogues are most often synthesized by precipitation in an aqueous solution. The reaction between the $[\text{Fe}(\text{CN})_6]^{3-}$ ferricyanide complex and the $[\text{Co}(\text{OH}_2)_6]^{2+}$ hexaaquacobalt(II) one leads to the forma-

(17) Bleuzen, A.; Escax, V.; Ferrier, A.; Villain, F.; Verdagner, M.; Münsch, P.; Itié, J.-P. *Angew. Chem., Int. Ed.* **2004**, *43*, 3728.

(18) Lüdi, A.; Güdel, H. U. *Structure and Bonding*; Springer-Verlag: Berlin, 1973; p 1.

(19) (a) Herrera, J. M.; Bachschmidt, A.; Villain, F.; Bleuzen, A.; Marvaud, V.; Wernsdorfer, W.; Verdagner, M. *Philos. Trans. R. Soc. A* **2008**, *366*, 127. (b) Verdagner, M.; Bleuzen, A.; Lescouëzec, R.; Marvaud, V.; Train, C. *L'actualité Chim.* **2005**, 290.

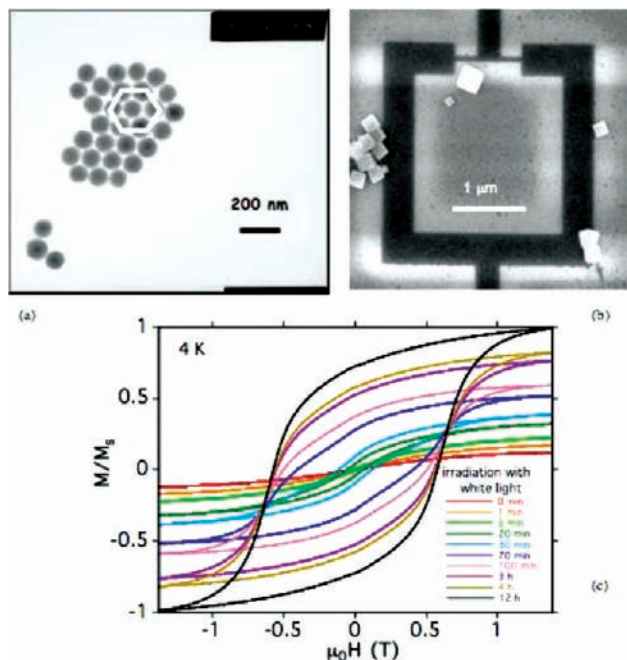


Figure 7. Examples of spherical (a) and cubic (b) particles obtained by variation of the concentration of the species present in the reaction medium. A cubic particle on a microSQUID (b). Photoinduced magnetization of a few nanoparticles (c) (ref 19 and courtesy of Bachschmidt and Wernsdorfer).

tion of a polycrystalline powder. The shape and to some extent the size of the particles depend on the concentration of the different species present in the reaction medium. Thus, by variation of their concentrations, it is possible to synthesize spherical or cubic objects (Figure 7). The size and shape essentially modify the photomagnetic response; the increase of the magnetization value under the same irradiation conditions is higher for spherical particles than for cubic ones, and the magnetization value is higher with smaller particles. For particle sizes higher than 70 nm, neither the Curie temperature nor the thermal relaxation temperature vary. Figure 7 evidences the transition from a dilute paramagnetic solid to a ferrimagnetic one on a few nanoparticles (measurement at 4 K in a microSQUID).¹⁹

2.3. Photoactive CoFe Octant. Recently, a discrete system that mimics the photomagnetic properties of the CoFe Prussian blue analogues has been reported.²⁰ This compound may be viewed as a stoichiometric molecular cube $\{\text{Fe}_4\text{Co}_4\}$ with alternation of Co and Fe at each corner and cyanide connectors on each edge. The cubes are well isolated by the presence of bulky ligands around the metallic centers: tetrapyrazolylborate (pzTp) for the Fe corners and 2,2,2-tris(pyrazolyl)ethanol for the Co corners (Figure 8a). With the use of spectroscopic, magnetic, and crystallographic methods, a fully reversible intramolecular electron transfer, interconverting LS $\text{Co}^{\text{III}}-\mu\text{-NC}-\text{LS Fe}^{\text{II}}$ and HS $\text{Co}^{\text{II}}-\mu\text{-NC}-\text{LS Fe}^{\text{III}}$ units as a function of the temperature or light has been demonstrated. At 30 K and under white-light irradiation, the magnetic response of the system is changing from an almost diamagnetic state to a paramagnetic state

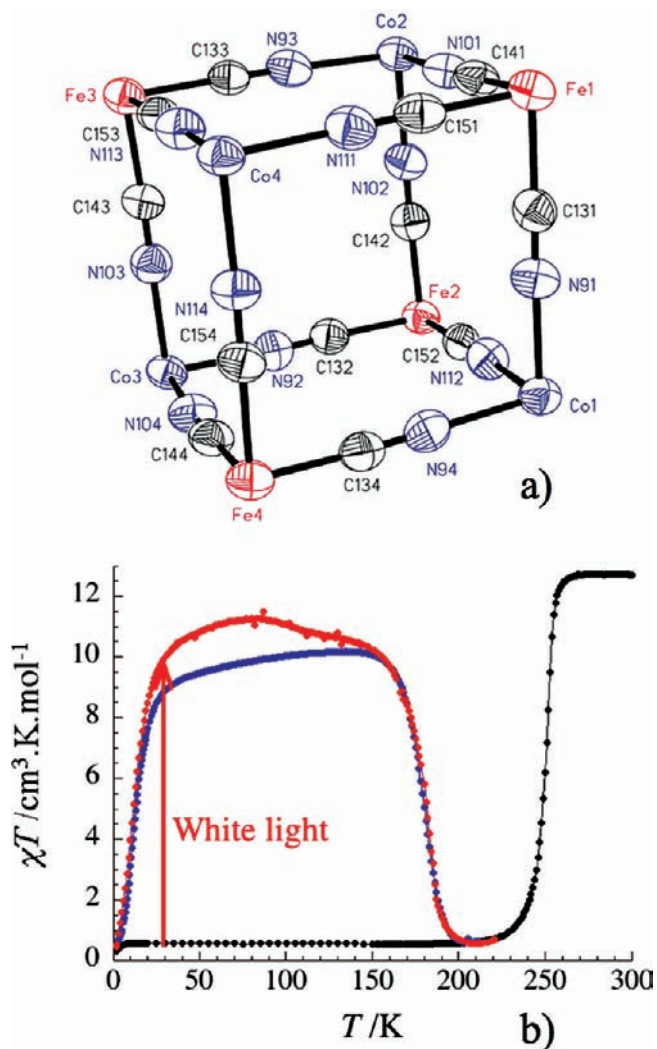


Figure 8. Molecular structure of the $\text{Fe}_4(\text{CN})_{12}\text{Co}_4$ box (the ligands around the metallic ions outside the box have been omitted for clarity) and $\chi_{MT} = f(T)$ in the dark state (black), in the light-induced state (red), and in the thermally quenched state (blue).

(Figure 8b). This intramolecular electron transfer can be circumvented via rapid thermal quenching. Moreover, the photostationary states obtained by light irradiation or rapid cooling, have higher lifetimes compared to the 3D networks.^{6,8,9}

This demonstrates the interest in purely molecular compounds for information storage because of their larger flexibility.

3. Photomagnetism in CuMo Systems

3.1. Photoactivity of Octacyanomolybdate Precursors (Including Systems in Solution). The photoreactivity of octacyanometalates was discovered early after the first synthesis of $\text{K}_4[\text{Mo}^{\text{IV}}(\text{CN})_8] \cdot 2\text{H}_2\text{O}$ in 1924.^{21–24} The systematic studies on photosubstitution and photoredox processes of $[\text{M}(\text{CN})_8]^{3-/4-}$ ions performed until the beginning of the 1990s resulted in the determination of mechanisms of photoreactions and identification of photoproducts, depending on the character of the lowest electronic excited state.

The aqueous solution absorption electronic spectra of octacyanometalates of Mo and W are presented in Table 1.

(20) Li, D.; Clérac, R.; Roubeau, O.; Harte, E.; Mathonière, C.; Le Bris, R.; Holmes, S. M. *J. Am. Chem. Soc.* **2008**, *130*, 252.

Table 1. Experimental Electronic Spectra of $[M(CN)_8]^{n-}$ ($M = Mo, W$)

octacyanometalate	$\nu_{\max}/\text{cm}^{-1}$	$\epsilon_{\max}/\text{M}^{-1}\cdot\text{cm}^{-1}$	assignment ^b
$[\text{Mo}(\text{CN})_8]^{3-}$	39 800	2687	LMCT
	36 800	2750	LMCT
	32 000	800	LMCT
	25 800	1357	LMCT
$[\text{Mo}(\text{CN})_8]^{4-}$	41 670	15540	MLCT
	37 400	1350	LF
	32 450	262	LF
	27 200	170	LF
	23 200	69	LF
	19 600	2.7	LF
$[\text{W}(\text{CN})_8]^{3-}$	41 490	2580	LMCT
	39 220	2634	LMCT
	28 010	1844	LMCT
$[\text{W}(\text{CN})_8]^{4-}$	40 169	25060	MLCT
	36 500	3000	LF
	33 000	520	LF
	27 000	251	LF
	23 000	111	LF
	19 900	4.8	LF

^a The experimental spectra (wavenumber and extinction coefficients) and assignment of the bands were taken from refs 25 and 26. ^b LMCT = ligand-to-metal charge transfer; MLCT = metal-to-ligand charge transfer; LF = ligand field.

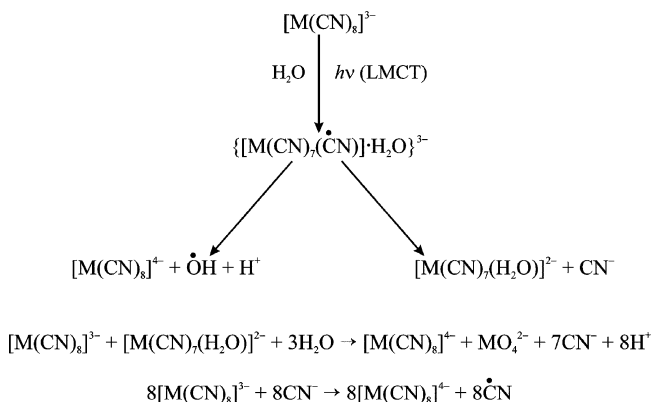
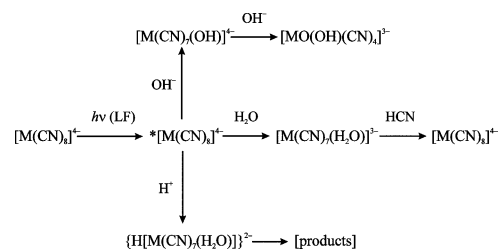
The character of the transitions has been established by Gołębiewski and co-workers using self-consistent charge and configuration method molecular orbitals²⁵ and by Ceulemans and Chibotaru thanks to CASPT2 calculations²⁶ performed for $[\text{Mo}(\text{CN})_8]^{3-}$, $[\text{Mo}(\text{CN})_8]^{4-}$, and $[\text{W}(\text{CN})_8]^{4-}$. The results indicate that, in aqueous media, in the case of $[\text{Mo}(\text{CN})_8]^{3-}$ the dodecahedral conformation (DD-8, D_{2d}) dominates the electronic spectrum, whereas for $[\text{M}(\text{CN})_8]^{4-}$, a dynamic equilibrium exists between the dodecahedron and square antiprism (SAPR-8).²⁶

Irradiation of the $[\text{M}(\text{CN})_8]^{3-}$ system in the lowest-energy ligand-to-metal charge transfer (LMCT) band at 355 nm causes the formation of $[\text{M}(\text{CN})_8]^{4-}$ ions (Scheme 1).²⁷

The photoprocess leading to $[\text{M}(\text{CN})_8]^{4-}$ occurs through two parallel pathways: (i) photoredox reaction giving directly the $[\text{M}(\text{CN})_8]^{4-}$ species as a photoproduct or (ii) photosubstitution giving the $[\text{M}(\text{CN})_7(\text{H}_2\text{O})]^{2-}$ primary photoproduct, followed by a series of secondary thermal redox reactions. The quantum yield of the photoredox process is found to be significantly higher ($\eta_p = 0.8$) than that of the photosubstitution reaction ($\eta_s = 0.2$).

The photoreaction of $[\text{M}(\text{CN})_8]^{4-}$ occurring under charge transfer to solvent (CTTS) excitation provides the formation of $[\text{M}(\text{CN})_8]^{3-}$ and release of the solvated electron (Scheme 2).²⁸

Irradiation in the ligand-field bands opens the pH-dependent substitutional photochemistry of $[\text{M}(\text{CN})_8]^{4-}$ ions

Scheme 1**Scheme 2****Scheme 3**

(Scheme 3).²⁹

Photolysis in an alkaline medium leads to the formation of $[\text{MO}(\text{OH})(\text{CN})_4]^{3-}$ passing through several intermediates with variable numbers of cyanide CN ligands. The photoprocess occurring in an acidic solution gives several products with different numbers of CN ligands formed from the protonated $\{[\text{H}[\text{M}(\text{CN})_7(\text{H}_2\text{O})]]^{2-}$ complex.

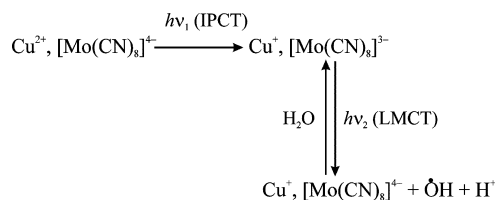
In the presence of d-electron metal cations and $[\text{M}(\text{CN})_8]^{4-}$, mixed-valence ion pairs are formed, characterized by the presence of an ion-pair charge-transfer (IPCT) transition in the visible part of the electronic spectrum of $[\text{M}(\text{CN})_8]^{4-}$ ions. This establishes the basis of the metal-to-metal charge-transfer (MMCT) photochemistry in ion pairs and cyano-bridged systems.³⁰ Irradiation of mixed-valence bimetallic compounds based on $[\text{Mo}^{\text{IV}}(\text{CN})_8]^{4-}$ and Fe^{2+} , Cu^{2+} , UO_2^{2+} , and VO^{2+} in the IPCT bands leads to the formation of valence isomers, as exemplified for the system $\text{Cu}^{2+}, [\text{Mo}(\text{CN})_8]^{4-}$ in Scheme 4.^{30b,e}

Excitation within the IPCT band causes the electron

- (21) Chilesotti, A. *Gazz. Chim. Ital.* **1904**, *34II*, 493.
 (22) Rosenheim, A.; Garfunkel, F.; Kohn, Z. *Z. Anorg. Allg. Chem.* **1910**, *65*, 166.
 (23) (a) Olsson, O. *Ber. Dtsch. Chem. Ges.* **1914**, *47*, 917. (b) Olsson, O. *Z. Anorg. Allg. Chem.* **1914**, *88*, 49.
 (24) Collenberg, O. *Z. Anorg. Allg. Chem.* **1924**, *136*, 245.
 (25) (a) Gołębiewski, A.; Kowalski, H. *Theor. Chim. Acta* **1968**, *12*, 293. (b) Gołębiewski, A.; Nalewajski, R. *Z. Naturforsch.* **1972**, *27a*, 1672.
 (26) (a) Hendrickx, M. F. A.; Chibotaru, L. F.; Ceulemans, A. *Inorg. Chem.* **2003**, *42*, 590. (b) Hendrickx, M. F. A.; Mironov, V. S.; Chibotaru, L. F.; Ceulemans, A. *Inorg. Chem.* **2004**, *43*, 3241.
 (27) (a) Sieklucka, B. *Inorg. Chim. Acta* **1991**, *186*, 179. (b) Sieklucka, B.; Samotus, A. *J. Photochem. Photobiol. A: Chem.* **1993**, *74*, 115.

- (28) (a) Waltz, W. L.; Adamson, A. W.; Fleishauer, P. D. *J. Am. Chem. Soc.* **1967**, *89*, 3923. (b) Shirom, M.; Siderer, Y. *J. Chem. Phys.* **1972**, *57*, 1013. (c) Kalisky, O.; Shirom, M. *J. Photochem.* **1977**, *7*, 215. (d) Vogler, A.; Losse, W.; Kunkely, H. J. C. S. *Chem. Commun.* **1979**, 187.
 (29) Leipoldt, J. G.; Basson, S. S.; Roodt, A. *Adv. Inorg. Chem.* **1993**, *40*, 241.
 (30) (a) Hennig, H.; Rehorek, A.; Ackermann, M.; Rehorek, D.; Thomas, Ph. *Z. Anorg. Allg. Chem.* **1983**, *496*, 186. (b) Hennig, H.; Rehorek, A.; Rehorek, D.; Thomas, Ph. *Inorg. Chim. Acta* **1984**, *86*, 41. (c) Hennig, H.; Benedix, R.; Billing, R. *J. Prakt. Chem.* **1986**, *328*, 829. (d) Billing, R.; Rehorek, D.; Salvetter, J.; Hennig, H. *Z. Anorg. Allg. Chem.* **1988**, *557*, 234. (e) Rehorek, D.; Rehorek, A.; Thomas, Ph.; Hennig, H. *Inorg. Chim. Acta* **1982**, *64*, L225. (f) Hennig, H.; Rehorek, A.; Rehorek, D.; Thomas, Ph.; Bätzold, D. *Inorg. Chim. Acta* **1983**, *77*, L11.

Scheme 4



transfer and formation of Cu^+ and $[\text{M}(\text{CN})_8]^{3-}$ species, followed by the photoreduction of octacyanometalate(V) entities after irradiation within its LMCT band. The very short lifetime τ of excited state $\text{Cu}^+, [\text{Mo}(\text{CN})_8]^{3-}$ at 295 K estimated as 3.60×10^{-9} s becomes 10^3 s at 93 K,^{30f} which lays the foundation of photomagnetic investigations of bimetallic cyano-bridged mixed-valence compounds based on Cu^{2+} and $[\text{Mo}(\text{CN})_8]^{4-}$ (see below, sections 3.2 and 3.3).

3.2. Photoactive CuMo Extended Networks. The use of octacyanometalates as building blocks to prepare new photosensitive coordination networks was developed after the discovery of the photomagnetic effect in the CoFe Prussian blue analogues (see section 2). The first system in this family to be described as a photomagnetically active compound was $[\text{Cu}^{\text{II}}(\text{H}_2\text{O})_2]_2[\text{Mo}^{\text{IV}}(\text{CN})_8] \cdot 4\text{H}_2\text{O}$ [$\text{Cu}_2\text{Mo}(\text{CN})_8$] in 2001.³¹ It was prepared in 1973, and it behaves as a paramagnet because of the presence of the isolated Cu^{2+} sites (d^9 , $S = 1/2$).³² The structural description of $[\text{Cu}^{\text{II}}(\text{H}_2\text{O})_2]_2[\text{Mo}^{\text{IV}}(\text{CN})_8] \cdot 4\text{H}_2\text{O}$ has been obtained thanks to X-ray spectroscopies, wide-angle X-ray scattering,³³ and comparison with the crystal structures of $\text{M}^{\text{II}}_2[\text{Mo}^{\text{IV}}(\text{CN})_8] \cdot x\text{H}_2\text{O}$, $\text{M} = \text{Mn}, \text{Fe},$ and Co analogues.³⁴ These data provided clear information about the 3D connectivity of $\text{Cu}-\text{NC}-\text{Mo}$ units in the network. After several hours of light irradiation in the range of the MMCT band at 480 nm and at 10 K, the system shows spontaneous magnetization below 20 K. The out-of-phase magnetic alternating current (ac) susceptibility (χ'') of the photoirradiated compound in the low-temperature region shows no frequency dependence (Figure 9), in agreement with magnetic ordering below 14 K.

The return to the initial state is estimated around 200 K and occurs in the paramagnetic region. The photomagnetic effect under visible light is interpreted by the formation of pairs of Mo^{V} ($S = 1/2$) and Cu^{I} ($S = 0$). The long-range magnetic ordering originates from the short-range ferromagnetic interactions between the photogenerated paramagnetic Mo^{V} and the residual Cu^{II} (Scheme 5, where the arrows correspond to spins $1/2$).

Recently, Ohkoshi et al. prepared a related compound $\text{Cs}_{0.5}\text{Cu}^{\text{II}}_{1.75}[\text{Mo}^{\text{IV}}(\text{CN})_8] \cdot 6\text{H}_2\text{O}$ by electrochemical synthesis in two different forms: crystals and films.³⁵ The crystal structure consists of a 3D cyano-bridged CuMo network

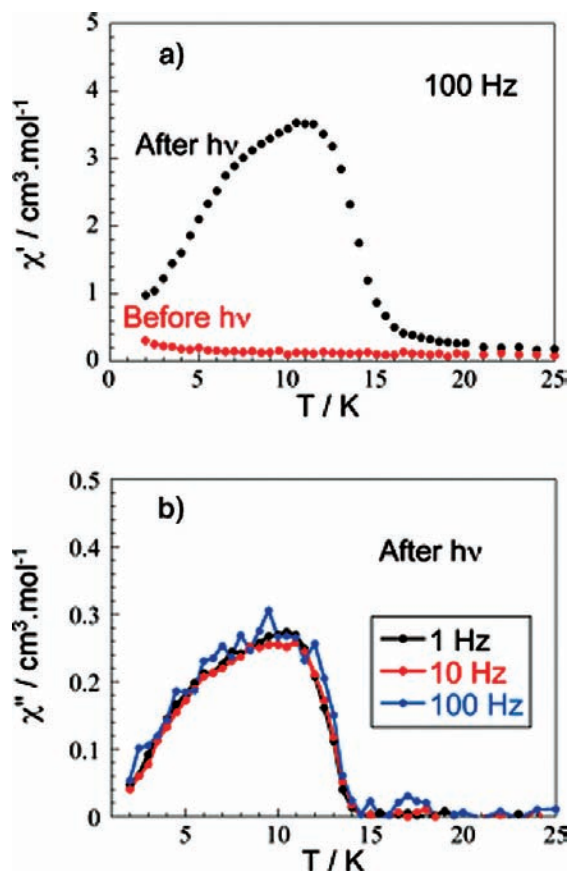
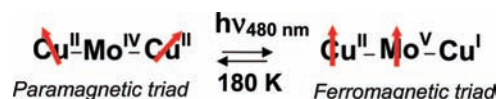


Figure 9. Thermal variation of the ac susceptibilities vs T : (a) real part of the susceptibility $\chi' = f(T)$ at 100 Hz, before and after irradiation; (b) imaginary part of the susceptibility $\chi'' = f(T)$ at different frequencies, after irradiation.

Scheme 5



(Figure 10). The differences with the previous network are (i) the presence of Cs^+ ions, which changes the Mo:Cu stoichiometry, and (ii) the presence of copper sites with two different coordination geometries (one is five-coordinate and square-pyramidal; the second is four-coordinate and square-planar). The compound, after irradiation with a blue light, shows a spontaneous magnetization at low temperature. The structural changes induced by light have been followed using XRD patterns. The observed modifications suggest that only square-pyramidal copper atoms are reduced in the photoirradiated compound.

Ma et al. reported X-ray spectroscopic studies in the two compounds CuMo presented above, in their irradiated phase. They demonstrate unambiguously the formation of Cu^{I} in the two solids and propose a structural deformation involving

(31) (a) Ohkoshi, S.; Machida, N.; Zhong, Z. J.; Hashimoto, K. *Synth. Met.* **2001**, *122*, 523. (b) Rombaut, G.; Verelst, M.; Golhen, S.; Ouahab, L.; Mathonière, C.; Kahn, O. *Inorg. Chem.* **2001**, *40*, 1151. (c) Ohkoshi, S.; Machida, N.; Abe, Y.; Zhong, Z. J.; Hashimoto, K. *Chem. Lett.* **2001**, 312. (d) Ohkoshi, S., private communication.

(32) MacKnight, F.; Haight, G. P. *Inorg. Chem.* **1973**, *12*, 3007.

(33) Ohkoshi, S.; Tokoro, H.; Hozumi, T.; Zhang, Y.; Hashimoto, K.; Mathoniere, C.; Bord, I.; Rombaut, G.; Verelst, M.; Cartier dit Moulin, C.; Villain, F. *J. Am. Chem. Soc.* **2006**, *128*, 270, and references cited therein.

(34) (a) Sra, A. K.; Rombaut, G.; Lahitete, F.; Golhen, S.; Ouahab, L.; Mathonière, C.; Yakhmi, J. V.; Kahn, O. *New J. Chem.* **2000**, *24*, 871. (b) Willemin, S.; Larionova, J.; Clérac, R.; Donnadiou, B.; Henner, B.; Le Goff, X. F.; Guérin, C. *Eur. J. Inorg. Chem.* **2003**, 1866. (c) Tuna, F.; Golhen, S.; Ouahab, L.; Sutter, J.-P. *C. R. Chimie* **2003**, *6*, 377.

(35) Hozumi, T.; Hashimoto, H.; Ohkoshi, S.-I. *J. Am. Chem. Soc.* **2005**, *127*, 3864.

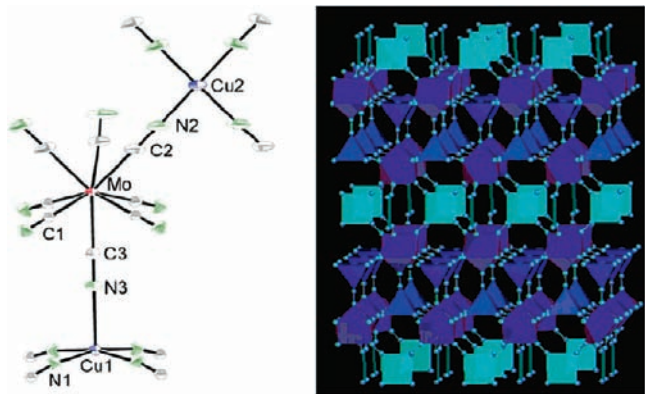


Figure 10. Crystal structure of $\text{Cs}_{0.5}\text{Cu}^{\text{II}}_{1.75}[\text{Mo}^{\text{IV}}(\text{CN})_8] \cdot 6\text{H}_2\text{O}$. Left: Coordination environments of the metal ions. Right: 3D network.

bending of the Cu–NC–Mo unit and tetrahedral deformation of the reduced site.³⁶

3.3. Molecular CuMo Complexes. 3.3.1. Description of the Systems. A similar switch effect based on the Cu–Mo couple has been observed as well in molecular species. Inspired by the photomagnetic 3D CuMo networks (section 3.2),^{36,37} photoswitchable HS molecules have been designed and synthesized and viewed as novel charge-transfer systems.^{37,38} The aim was to modify, in a reversible process, the magnetic properties of molecular entities using, as external perturbation, a photonic irradiation.

In a continuation of the synthetic strategy previously described for polynuclear compounds based on hexacyanometalate chemistry,^{39–41} tri- and heptanuclear complexes based on octacyanometalate diamagnetic Mo^{IV} and Cu^{II} precursors in the presence of blocking ligands have first been described (Figure 11).^{42,43}

These polynuclear complexes, $[\text{Mo}(\text{CN})_2\{\text{CN-Cu}(\text{bipy})_2\}_2]^0$ and $[\text{Mo}(\text{CN})_2\{\text{CN-Cu}(\text{tren})\}_6](\text{ClO}_4)_8$, denoted as $\text{MoCu}_2(\text{bipy})$ and $\text{MoCu}_6(\text{tren})$, respectively, are obtained by the addition of an octacyanomolybdate(IV) solution to the mononuclear Cu^{II} complex generated in situ from the ligand 2,2′-bipyridine (bipy) or tris(2-aminoethyl)amine (tren) and Cu^{II} salts. Both compounds have optical absorptions in the UV range corresponding to ligand-field bands of the $[\text{Mo}(\text{CN})_8]^{4-}$ chromophore and in the visible range attributed to the d–d transition of the Cu^{II} ions. They exhibit as well a band around 500 nm corresponding to an intervalence charge transfer (IVCT) corresponding to a $\text{Cu}^{\text{II}}\text{–Mo}^{\text{IV}} \rightarrow$

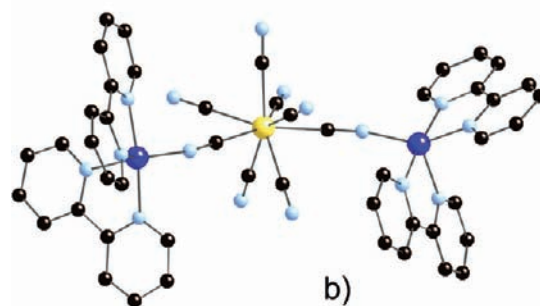
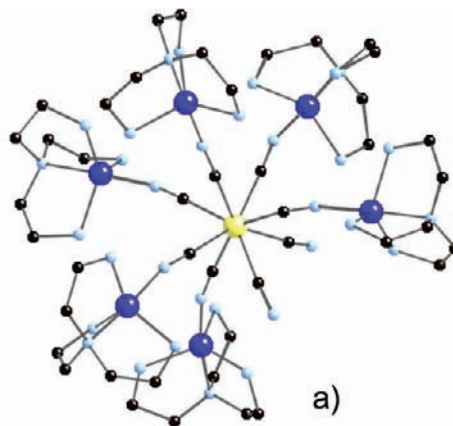


Figure 11. Crystallographic structures of the molecular entities of a) $[\text{Mo}(\text{CN})_2\{\text{CN-Cu}(\text{tren})\}_6]^{8+}$ and b) $[\text{Mo}(\text{CN})_2\{\text{Cu}(\text{bipy})_2\}_2]^0$.

$\text{Cu}^{\text{I}}\text{–Mo}^{\text{V}}$ transition. This wavelength is used for irradiation. The two compounds exhibit photoinduced magnetic modifications in the solid state.

3.3.2. Photomagnetic Properties. Before irradiation, the magnetic properties of the two compounds were measured as the temperature dependence of the magnetic susceptibility and the field dependence of the magnetization (at 10 K). No significant magnetic exchange interactions were observed for the two molecules formed by Cu^{II} ions ($S_{\text{Cu}} = 1/2$) separated by the diamagnetic Mo^{IV} ion ($S_{\text{Mo}} = 0$). The curves correspond to what is expected for isolated paramagnetic Cu ions and fit perfectly the Brillouin function for noninteracting $S = 1/2$ spins.

We point out first the importance of the irradiation conditions and especially the selectivity of the wavelength in the photoinduced process. The first photomagnetic experiments on the trinuclear complex $\text{MoCu}_2(\text{bipy})$ were performed under UV light excitation (337–356 nm)^{19a} and indicated irreversible changes. Recent investigations on this compound with irradiation in the range of the IVCT band observed in its optical spectra (488 nm) have demonstrated reversible modification.⁴³ In this specific case, the identification of the IVCT band is difficult because of the large overlap with the d–d transitions of Cu^{2+} .

For the heptanuclear complex $\text{MoCu}_6(\text{tren})$, after 10 h of irradiation at 406 nm, the $\chi T = f(T)$ curve changes drastically and is consistent with strong ferromagnetic interaction between the spin carriers. After room temperature was

(36) Ma, X.-D.; Yokoyama, T.; Hozumi, T.; Hashimoto, K.; Ohkoshi, S. *Physical Review B* **2005**, *72*, 094107.

(37) Dei, A. *Angew. Chem., Int. Ed.* **2005**, *117*, 1184.

(38) Sato, O.; Tao, J.; Zhang, Y.-Z. *Angew. Chem., Int. Ed.* **2007**, *46*, 2152.

(39) Marvaud, V.; Decroix, C.; Scüller, A.; Guyard-Duhayon, C.; Vaissermann, J.; Gonnet, F.; Verdaguer, M. *Chem.–Eur. J.* **2003**, *9* (8), 1677.

(40) Marvaud, V.; Decroix, C.; Scüller, A.; Tuyéras, F.; Guyard-Duhayon, C.; Vaissermann, J.; Marrot, J.; Gonnet, F.; Verdaguer, M. *Chem.–Eur. J.* **2003**, *9* (8), 1692.

(41) Tuyéras, F.; Scüller, A.; Duhayon, C.; Hernandez-Molina, M.; Fabrizi de Biani, F.; Verdaguer, M.; Mallah, T.; Wernsdorfer, W.; Marvaud, V. *Inorg. Chim. Acta* **2008**, *361*, 3505.

(42) Herrera, J.-M.; Marvaud, V.; Verdaguer, M.; Marrot, J.; Kalisz, M.; Mathonière, C. *Angew. Chem., Int. Ed.* **2004**, *43* (41), 5468.

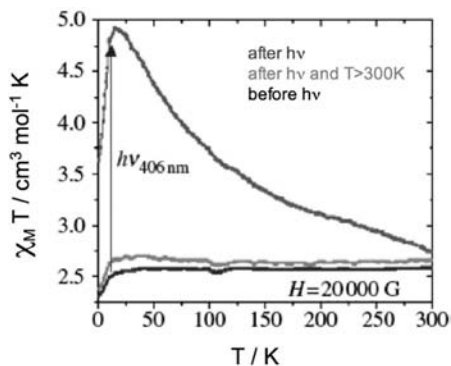


Figure 12. Photomagnetic HS $\text{MoCu}_6(\text{tren})$ molecule: photoinduced change in the $\chi_M T$ product.

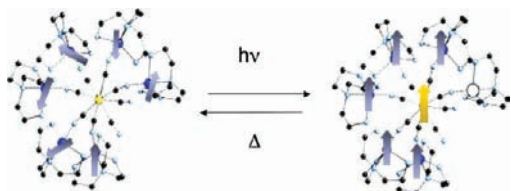


Figure 13. Scheme of the photoinduced electron transfer and of the mixed-valence photoexcited state $\text{Mo}^{\text{V}}\text{Cu}^{\text{I}}\text{Cu}^{\text{II}}_5$.

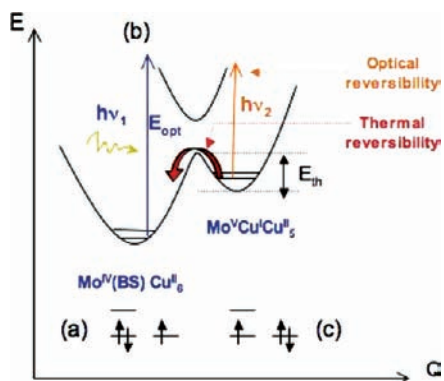


Figure 14. Potential energy diagram in the solid state for $\text{MoCu}_6(\text{tren})$ viewed as a class II mixed-valence compound. The initial state, $\text{Mo}^{\text{IV}}\text{Cu}^{\text{II}}_6$ (a), is paramagnetic. Irradiating with blue light ($h\nu_1$) excites $\text{MoCu}_6(\text{tren})$ to the charge-transfer state (b); then the complex forms a mixed-valence isomer, $\text{Mo}^{\text{V}}\text{Cu}^{\text{I}}\text{Cu}^{\text{II}}_5$, which is trapped at low temperature (c). The energy barrier (E_{th}) is around 300 K.

reached at 300 K, the paramagnetic behavior is observed again, indicating unambiguously the reversibility of the process (Figure 12).

This effect can be explained by a photoinduced electron transfer from Mo^{IV} (d^2 , $S = 0$) to Cu^{II} (d^9 , $S = 1/2$), leading to Mo^{V} (d^1 , $S = 1/2$) and Cu^{I} (d^{10} , $S = 0$) and the formation of a paramagnetic-centered species: $\text{Mo}^{\text{V}}\text{Cu}^{\text{I}}\text{Cu}^{\text{II}}_5$ with $S = 3$ (Figure 13).

The phenomenon is thermally and optically reversible. The reverse process appears at 300 K when thermally induced and at 840 nm when optically provoked.^{31d} The photoinduced metastable state has a long lifetime of at least several days at low temperature. The switch process appears indefinitely active (according to experiments performed over several days and many turns over). The two kinds of experimental observations reveal a long-lived, robust, metastable state with a high activation energy barrier between the metastable and ground states. The exact determination of the barrier energy

and the nature of the metastable state remains a challenge. In particular, the kinetics of relaxation might change from one compound to another. To explain the formation and stability of the long-lived metastable-state high relaxation temperature, it has been suggested that (i) there is a significant local reorganization around Cu^{I} , (ii) the molybdenum coordination sphere should adopt an intermediate geometry between the square antiprism and dodecahedron, where the d_{z^2} and $d_{x^2-y^2}$ orbitals are close in energy,⁴⁴ (iii) there is no orbital overlap between magnetic orbitals of molybdenum and copper, and (iv) the observed photomagnetic effect can be described by the schematic potential diagram of a class II mixed-valence compound (Figure 14).^{45,46}

The local geometry structure of the possible metastable state for the $[\text{Mo}^{\text{IV}}(\text{CN})_2(\text{CN}-\text{Cu}^{\text{II}}\text{L})_6]$ species has been optimized with the density functional theory method.⁴⁷ The calculation results indicate that the trigonal-bipyramidal coordination environment surrounding one Cu^{II} ion changes to tetrahedral coordination around the Cu^{I} ion after light irradiation. The magnetic properties calculated by using different theoretical approaches reveal that the HS metastable state is a long-lived $S = 3$ charge-transfer excited state, in agreement with the present experimental results.^{48,49}

3.3.3. Demonstration of the Electron Transfer. In order to demonstrate the photoinduced electron transfer, several spectroscopic experiments have been performed. The main results have been obtained by X-ray absorption spectroscopy, a useful technique to probe the local structural and electronic environment of specific ions. The EXAFS allows one to determine the distances between the absorber and the neighboring first shells. X-ray absorption near-edge structure (XANES) is sensitive to the electronic structure of the absorber (oxidation and spin states, local symmetry, etc.). We used it before and after irradiation at low temperature.^{19a,50}

Reference compounds of Mo^{IV} , Mo^{V} , Cu^{II} , and Cu^{I} have first been analyzed. The Mo L_3 edge spectra are presented on Figure 15. Before irradiation, the XANES spectrum recorded for $\text{MoCu}_6(\text{tren})$ is similar to the one obtained for the octacyanometalate precursor $[\text{Mo}(\text{CN})_8]^{4-}$ in which the molybdenum is Mo^{IV} (d^2 , $S = 0$). After irradiation (410 nm), the spectrum changes: (i) a new peak appears at 2522 eV [due to partially occupied orbitals (d^1) compared to the initial diamagnetic d^2 configuration] and (ii) the major edge is shifted to higher energy, as was expected with an increase of the oxidation state of the element. The spectrum after irradiation is compared to a dinuclear $\text{Mo}^{\text{V}}\text{Cu}^{\text{II}}$ reference compound. It is in good agreement with a Mo^{V} oxidation

(43) Mathonière, C.; Kobayashi, H.; Le Bris, R.; Kaiba, A.; Bord, I. C. R. *Chimie* **2008**, *11*, 665.

(44) Ruiz, E., private communication.

(45) Marcus, R. A. *Angew. Chem., Int. Ed. Engl.* **1993**, *32*, 1111.

(46) Hush, N. S. *Coord. Chem. Rev.* **1985**, *64*, 135.

(47) Wang, B.; Wang, M.; Chen, Z. *Polyhedron* **2007**, *26*, 2054.

(48) Raghunathan, R.; Ramasesha, S.; Mathonière, C.; Marvaud, V. *Phys. Rev. B* **2006**, *73*, 045131.

(49) Raghunathan, R.; Ramasesha, S.; Mathonière, C.; Marvaud, V. *Phys. Chem. Chem. Phys.* **2008**, *10*, 5469.

(50) Marvaud, V., work in progress.

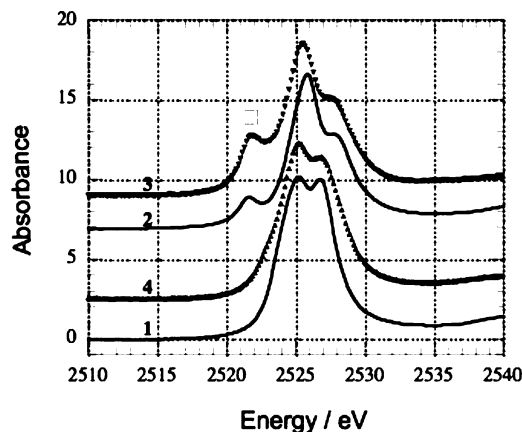


Figure 15. Mo L_{3} edge spectra: **1**, $\text{Mo}^{\text{IV}}\text{-Cu}^{\text{II}}_6(\text{tren})$ molecule (10 K); **2**, a $\text{Mo}^{\text{V}}\text{-[Cu}^{\text{II}}\text{L}]_1$ model (10 K); **3**, $\text{Mo}^{\text{V}}\text{-Cu}^{\text{I}}_1\text{Cu}^{\text{II}}_5(\text{tren})$ molecule after irradiation (10 K); **4**, $\text{Mo}^{\text{IV}}\text{-Cu}^{\text{II}}_6(\text{tren})$ molecule after irradiation at 10 K and relaxation at room temperature. The \square points out the presence of an electronic vacancy in the lowest-lying d orbital of the Mo^{V} model and of the molecule in the photoinduced metastable state.

degree spectrum. It demonstrates that irradiation at low temperature creates a hole in the lowest occupied d orbitals of Mo^{IV} . After returning at room temperature, the initial spectrum is recovered, showing that the process is fully reversible.

The reduction of the copper site is more difficult to characterize at the Cu K and $L_{2,3}$ edges because photoreduction can occur under intense synchrotron light. Indeed, after too long and too intense irradiation, photoreduction of the Cu ion, associated with an irreversible flip of the cyanide ligand and the formation of a $[\text{NC-Cu}^{\text{I}}(\text{ligand})]$ fragment, can be observed. When irradiation damage is avoided, the results have been confirmed by similar XANES experiments, recorded at the Cu K and $L_{2,3}$ edges, indicating the presence of Cu^{I} after irradiation and the reversibility of the photoinduced process.

Two bimetallic molecules have been investigated by XMCD measurements at the Mo $L_{2,3}$ edges— $[\text{Mo}(\text{CN})_2(\text{CN-CuL})_6]^{8+}$, with L being tris(2-amino)ethylamine, and $[\text{Mo}(\text{CN})_6(\text{CN-CuL})_2]$, with L being N,N' -dimethylethylenediamine—leading to fruitful information on the spin density and on the atomic magnetic moments (Figure 16). In both cases, before irradiation, the XMCD signal is null, as was expected for diamagnetic Mo^{IV} ($S = 0$). After irradiation, a XMCD signal appears, which directly demonstrates the formation of spin density on the Mo ion. After room temperature is reached, the signal disappears, indicating clearly the reversibility of the photoinduced process. The XMCD experiments allow one to evidence as well an additional X-ray photoinduced excited state based on HS Mo^{IV} ($S = 1$).⁵¹ The geometry of the molybdenum (intermediate between the square antiprism and dodecahedron) might explain the formation and stability of a low-lying triplet excited state, considering that such a geometry allows

a triplet state even in the ground state (with the d_{z^2} and $d_{x^2-y^2}$ orbitals being close in energy).

3.3.4. Lifetime of the Metastable State. The photo-switching effect within the heterobimetallic complexes has been analyzed by X-band electron paramagnetic resonance (EPR) experiments, at low temperature, under light excitation. Before irradiation, the samples show only a broad singlet line in X-band EPR, in good agreement with the presence of isolated Cu^{II} ions. Under irradiation (blue laser, 488 nm), performed at 10 K, the EPR signal disappears, suggesting that all spins are magnetically coupled. After irradiation (correlated to the IVCT band), two different processes are observed according to the nature of the compounds: (i) in $\text{MoCu}_6(\text{tren})$, the metastable state is a long-lived state and persists up to room temperature (i.e., $T_{\text{relax}} = 300$ K); (ii) in $\text{MoCu}_2(\text{bipy})$, the metastable state is a short-lived state and relaxes when the light is switch off ($T_{\text{relax}} = 4$ K). These experiments suggest that, despite their chemical analogies (based on a Mo-CN-Cu unit), the complexes do not behave in an identical way: different lifetimes and different relaxation kinetics of the metastable states are observed. The results are directly correlated to the mixed-valence species $\text{Mo}^{\text{V}}\text{-(CN-Cu}^{\text{I}}\text{)(CN-Cu}^{\text{II}}\text{)}$, which are differently trapped at low temperature as a function of (i) ligand flexibility and (ii) orbital overlap, having a direct influence on the electronic coupling (V_{ab}) and the energy barrier (E_{th}).^{50,52}

3.3.5. Cu–Mo Unit as a Switch in Complex Systems. Integrating the above-mentioned Cu–Mo light-activable behaviors within a single smart molecule is naturally the next step toward photoswitchable molecular nanomagnets. Following an approach adapted from the modular synthetic strategy,^{41–43} one such promising entity has been recently described.⁵³ Keeping the working principle of the switching effect, that is, the photoinduced electron transfer between the Mo^{IV} core and one of the cyano-bridged dangling Cu^{II} ions ($\text{Mo}^{\text{IV}}\text{-Cu}^{\text{II}} \rightarrow \text{Mo}^{\text{V}}\text{-Cu}^{\text{I}}$), a Ni^{II} -based building block was incorporated in the inorganic assembly. Thus, a heterotrimetallic chain, $[(\text{Ni}^{\text{II}}(\text{cyclam}))(\text{Mo}^{\text{IV}}\text{-(CN)}_8)_2(\text{Cu}^{\text{II}}(\text{Me}_2\text{en})_2)_7]^{8+}$, denoted NiMo_2Cu_7 , has been obtained (Figure 17).

Thus, before irradiation, the complex behaves as a paramagnetic species containing isolated magnetic species as expected for a Mo^{IV} metallic cation (diamagnetic) surrounded by isolated Ni^{II} and Cu^{II} ions. After irradiation, the magnetic properties are consistent in a first approximation with a HS metastable state ($S = 5/2$). The effect is explained by a photoinduced electron transfer from Mo^{IV} to Cu^{II} , leading to Mo^{V} and Cu^{I} , with magnetic exchange interactions between the residual spin carriers. Moreover, the photomagnetic effect persists until 120 K. It is thermally reversible. More details can be found in ref 53. Considering long-range interaction, the compound might be described as the first example of a fully reversible photomagnetic chain. It

(51) Arrio, M. A.; Long, J.; Cartier dit Moulin, C.; Marvaud, V.; Bachschmidt, A.; Rogalev, A.; Mathonière, C.; Wilhelm, F. *Saintcavit*, P., submitted.

(52) Ruiz, E.; Alvarez, S., work in progress.

(53) Long, J.; Chamoreau, L.-M.; Mathonière, C.; Marvaud, V. *Inorg. Chem.* **2009**, *48*, 22.

(54) Bogani, L.; Wernsdorfer, W. *Nat. Mater.* **2008**, *7*, 179.

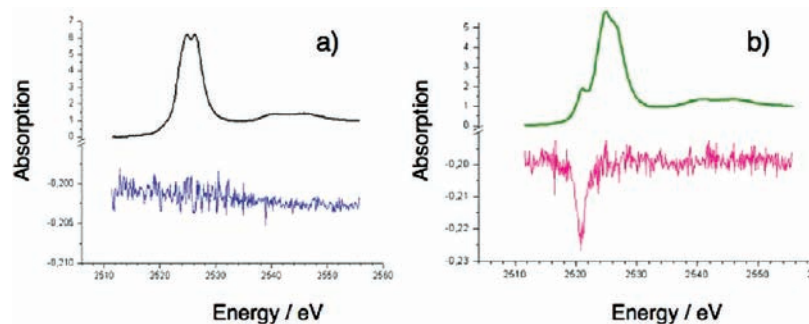


Figure 16. Absorption spectra and XMCD signals at the Mo L_3 edge of $\text{MoCu}_6(\text{tren})$ recorded at $T = 7$ K and $H = \pm 6$ T: (a) before irradiation; (b) after irradiation.

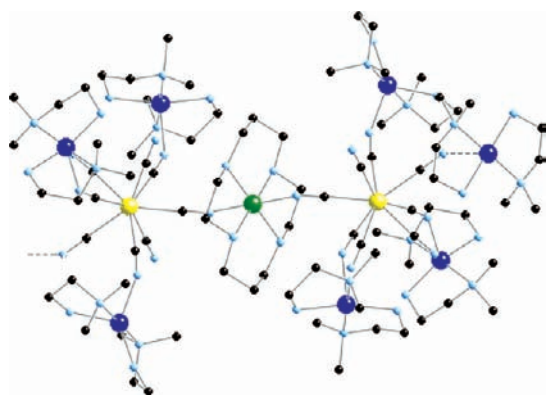


Figure 17. Single-crystal X-ray structure of the $[\text{NiMo}_2\text{Cu}_7]$ chain.

combines the CuMo-based switching effect, large spin, and structural anisotropy. It demonstrates the flexibility of the system for further studies, including switchable single-chain magnets, presenting electronic anisotropy and slow relaxation of the magnetization, not yet obtained. The result opens the field of stable heterotrimetallic structures built by the reaction of (photoswitchable) molecular heterodimetallic complexes and assembling building blocks. Through a combination of suitable properties (switching effect, spin, and anisotropy), this work traces the path to photoswitchable nanomagnets.

The molecular CuMo photoswitch is rich in applications. Several other molecular systems are now under study,⁵⁰ and theoretical analyses of the phenomenon are in progress.⁵² On the way to molecular spintronics,⁵⁴ these compounds might be viewed as photomagnetic molecular devices,⁵⁵ prototypes of photochemical molecular devices.⁵⁶

3.4. Photoactive Nanoparticles. The preparation of nanoparticles based on the photomagnetic CuMo networks has been reported with the use of matrix polymer poly(vinylpyrrolidone) (PVP) to confine growth of the particles during their formation. This system has been studied as an optically transparent film containing 19% nanorods of the photoactive material.⁵⁷ Its photomagnetic properties are described in another contribution of this *Inorganic Chemistry Forum*.⁵⁸

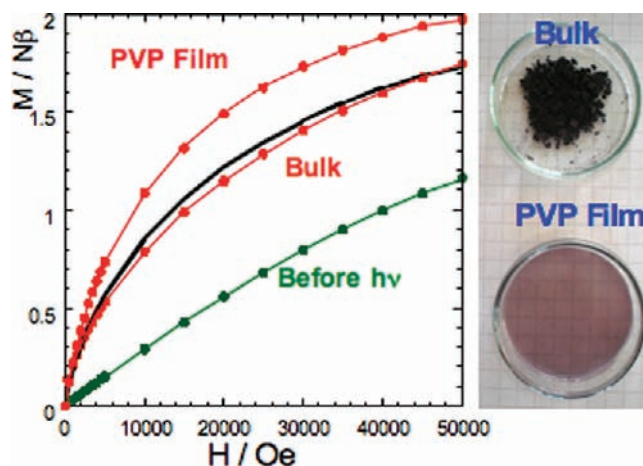


Figure 18. Comparison of the magnetization at 5 K before (green) and after irradiation (red) in the bulk and in the film of the $\text{Cu}_{12}\text{Mo}^{\text{IV}}(\text{CN})_8$ network. The black line corresponds to $M = 0.75 * M(\text{PVP film})$, close to M (bulk).

We recall, however, the two main conclusions related to this nanostructured material: (1) the photoconversion yield of the electron transfer is improved in the film (Figure 18; 100% of photogenerated $\text{Cu}^{\text{II}}\text{Mo}^{\text{V}}\text{Cu}^{\text{I}}$ triads for the nanorods compared to a 70% yield in the bulk material); this improvement is attributed to a better penetration of the light in the film than in the bulk; (2) no magnetic ordering after light irradiation is observed. The material after irradiation remains in a paramagnetic state because of the nanometric size of the rods.

A new nanostructured material has been obtained under conditions similar to those of the nanosized $\text{Cu}_2\text{Mo}(\text{CN})_8$ with the Ni ion.⁵⁹ The formula of this new material is $\text{NiCuMo}(\text{CN})_8$ coated with a PVP shell. It consists of small spherical nanoparticles of diameter of around 3 nm. The anisotropic nature of the Ni^{2+} ion has important consequences on the photomagnetic properties of the material. Actually, the nanoparticles after irradiation behave as superparamagnetic single-domain clusters of about $55 \pm 8 \text{ Ni}^{\text{II}}\text{Cu}^{\text{I}}\text{Mo}^{\text{V}}$ units ($S_{\text{max}} = 82 \pm 12$).

4. Photomagnetism Using Other Bimetallic Pairs

We quote here a few works implying some other metallic pairs than the ones considered before, Co–Fe or Cu–Mo.

(55) Ciofini, I.; Lainé, P. P.; Zamboni, M.; Daul, C. A.; Marvaud, V.; Adamo, C. *Chem.—Eur. J.* **2007**, *13* (19), 5360.

(56) Balzani, V. *Photochem. Photobiol. Sci.* **2003**, *2* (5), 459.

(57) Catala, L.; Mathonière, C.; Gloter, A.; Stephan, O.; Gacoin, T.; Boilot, J.-P.; Mallah, T. *Chem. Commun.* **2005**, 746.

(58) Catala, L.; Volatron, F.; Brinzei, D.; Mallah, T. Functional Coordination Nanoparticles. *Inorg. Chem.*, present issue.

(59) Brinzei, D.; Catala, L.; Mathonière, C.; Wernsdorfer, W.; Gloter, A.; Stephan, O.; Mallah, T. *J. Am. Chem. Soc.* **2007**, *129*, 746.

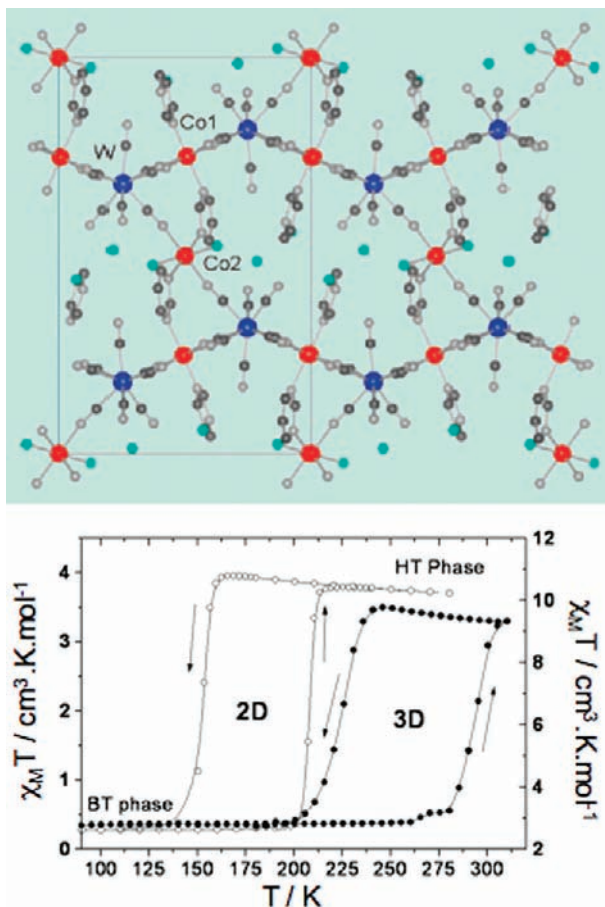


Figure 19. (a) Crystal structure of the 3D network $[\{\text{Co}^{\text{II}}(\text{pyrimidine})_2\}_2\{\text{Co}^{\text{II}}(\text{H}_2\text{O})_2\}\{\text{W}^{\text{V}}(\text{CN})_8\}_2]\cdot 4\text{H}_2\text{O}$. (b) Thermal-induced charge transfer for the 2D network $\text{Cs}\{\{\text{Co}^{\text{II}}(3\text{-cyanopyridine})_2\}\{\text{W}^{\text{V}}(\text{CN})_8\}\}\cdot \text{H}_2\text{O}$ (○) and the 3D network (●) between the high-temperature (HT) $\text{Co}^{\text{II}}\text{W}^{\text{V}}$ phase and the low-temperature (LT) $\text{Co}^{\text{III}}\text{W}^{\text{IV}}$ phase.

4.1. Photoactive Molecular Manganese Octacyanometallates. Two other molecular compounds containing octacyanometallates have been prepared with Mn^{2+} and bipy ligands, $[\text{Mn}^{\text{II}}(\text{bipy})_2]_4[\text{M}(\text{CN})_8]_2$. The structure consists of hexanuclear clusters with a metallic core: Mn_4Mo_2 and Mn_4W_2 . Both show photomagnetic properties that are maintained at room temperature for the Mo analogue. In this nonreversible case, an XPS analysis of the photoproduct has shown the formation of Mn^{I} and Mo^{V} . It has been interpreted in terms of a reductive quenching from the excited state through an intramolecular electron transfer in the cluster $[\text{Mn}^{\text{II}}(\text{bipy})_2]_4[\text{M}(\text{CN})_8]_2$.⁶⁰

4.2. Photoactive Co–W Extended Networks. $[\text{W}^{\text{V}}(\text{CN})_8]^{3-}$ is also an efficient building block for photomagnetic systems when it is associated with the Co^{2+} ion and derivatives of pyridine ligands. Actually, two different structures have been reported by Ohkoshi et al.: one corresponds to a 2D network, formula $\text{Cs}\{\{\text{Co}^{\text{II}}(3\text{-cyanopyridine})_2\}\{\text{W}^{\text{V}}(\text{CN})_8\}\}\cdot \text{H}_2\text{O}$,⁶¹ and the other to a 3D network, formula $[\{\text{Co}^{\text{II}}(\text{pyrimidine})_2\}_2\{\text{Co}^{\text{II}}(\text{H}_2\text{O})_2\}\{\text{W}^{\text{V}}(\text{CN})_8\}_2]\cdot 4\text{H}_2\text{O}$.⁶² The structures consist of layers where Co and W ions are alternated. In the 2D network, the Co ion is surrounded by four cyano ligands and two terminal cyanopyridine ligands. In the 3D network

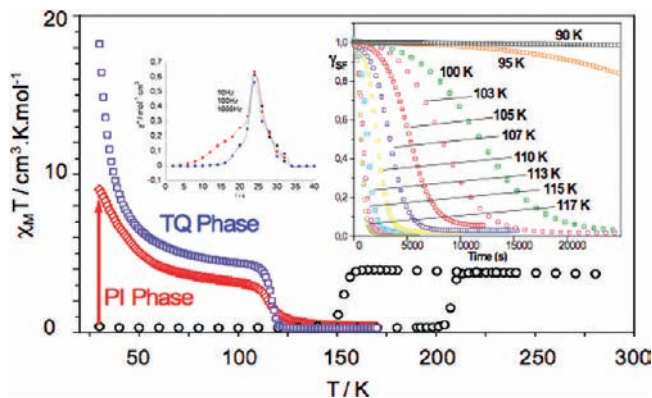


Figure 20. Stable (dark) and metastable states (red, light-induced; blue, thermally quenched (TQ) state) for $\text{Cs}\{\{\text{Co}^{\text{II}}(3\text{-cyanopyridine})_2\}\{\text{W}^{\text{V}}(\text{CN})_8\}\}\cdot \text{H}_2\text{O}$. Insets: (left) thermal dependence of the out-of-phase susceptibility at different frequencies of the TQ state in the 4–40 K range; (right) time dependence of the magnetic signal of the TQ phase in the 90–117 K range.

(Figure 19, top), the Co ion in the layer is surrounded by four cyanido ligands and two bridging pyrimidine ligands connecting the layers through the second site of cobalt, made of two cyanido, two water, and two pyrimidine. The pyrimidine plays the role of linker between the layers (Figure 19).

The properties of these networks are close to those of the alkali derivatives of CoFe Prussian blue analogues. When the temperature is lowered, a thermal-induced charge transfer converts the high-temperature paramagnetic pairs Co^{II} (d^7 HS, $S = 3/2$)– $\text{NC}-\text{W}^{\text{V}}$ (d^1 , $S = 1/2$) into the low-temperature diamagnetic pairs Co^{III} (d^6 LS, $S = 0$)– $\text{NC}-\text{W}^{\text{IV}}$ (d^2 , $S = 0$) with a hysteresis loop of 55 K for the 2D network and of 70 K for the 3D network (Figure 19b, right). At low temperature, when the compounds are irradiated with red light, the metastable pairs Co^{II} (d^7 HS, $S = 3/2$)– $\text{NC}-\text{W}^{\text{V}}$ (d^1 , $S = 1/2$) are generated and lead to ferromagnetic ordering below 30 K (2D network) and 40 K (3D network). Accompanying the charge transfer, an important change of color occurs, from a red color at high temperature to a blue color at low temperature. Yokohama et al. reported X-ray spectroscopy studies of the 2D network.⁶³ They showed an increase of the Co–N bond lengths of 0.17 Å in the light-induced phase compared to the low-temperature phase. Note that, in another related 3D network, formula $[\{\text{Co}^{\text{II}}(\text{pyrimidine})_2\}_2\{\text{Co}^{\text{II}}(\text{H}_2\text{O})_2\}\{\text{W}^{\text{V}}(\text{CN})_8\}_2]\cdot (\text{pyrimidine})_2\cdot 2\text{H}_2\text{O}$, neither thermal- nor light-induced phase transition occurs.⁶⁴ This is a consequence of a decrease of the crystal field strength around the Co due to substitution of one pyrimidine by one water molecule. Le Bris et al. realized a detailed study for the 2D network of the metastable state generated by red light irradiation or by rapid cooling.⁶⁵ Both states show a magnetic

(61) Arimoto, Y.; Ohkoshi, S.-I.; Zhang, Z. J.; Seino, H.; Mizobe, Y.; Hashimoto, K. *J. Am. Chem. Soc.* **2003**, *125*, 9240.

(62) Ohkoshi, S.-I.; Ikeda, S.; Hozumi, T.; Kashiwagi, T.; Hashimoto, K. *J. Am. Chem. Soc.* **2006**, *128*, 5320.

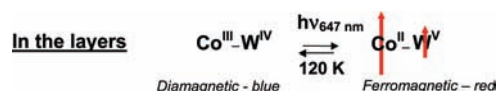
(63) Ohkoshi, S.-I.; Hamada, Y.; Matsuda, T.; Tsunobuchi, Y.; Tokoro, H. *Chem. Mater.* **2008**, *20*, 3048.

(64) Yokoyama, T.; Okamoto, K.; Ohta, T.; Ohkoshi, S.; Hashimoto, K. *Phys. Rev. B* **2002**, *65*, 064438.

(65) Le Bris, R.; Mathonière, C.; Létard, J.-F. *Chem. Phys. Lett.* **2006**, *426*, 380.

(60) Mathonière, C.; Podgajny, R.; Guionneau, P.; Labrugère, C.; Sieklucka, B. *Chem. Mater.* **2005**, *17*, 442.

Scheme 6



ordering, as shown by the ac frequency dependence of the thermally quenched state (Figure 20). Moreover, they reported a magnetic study of relaxations at fixed temperature from the metastable state to the low-temperature phase. The relaxation of the magnetic signal at fixed temperature presents a sigmoidal shape, a typical behavior for cooperative spin-crossover compounds (Figure 20).⁶⁶

The photomagnetic effect in these CoW networks may be summarized by a charge transfer taking place in the layer (Scheme 6). In the scheme, the arrows correspond to a spin $1/2$ on the W site and a spin $3/2$ on the Co site.

5. Conclusion

We have presented some examples of bimetallic photo-magnetic systems, implying an electron transfer from one metal to another, and discussed the present state of the art in this field. We are convinced that the systematic check of the presence of intervalence bands in bimetallic systems and the investigation of the appropriate photomagnetic response will provide in the future many more examples of such photoinduced molecular switches within a bimetallic pair. Besides this extension of the domain to other systems, two

trends can be noted: one toward more complex systems and the other toward nanosized systems. For more complex systems, if the bimetallic switch is inserted into a trimetallic network, the path is open for commutating the magnetic properties of the whole system. This needs, of course, to overcome entropic and kinetic hindrances to get structurally ordered materials. When combined with anisotropy, photo-magnetic systems will be able to provide switchable single-molecule and single-chain magnets. Going to nanosized systems and controlling the size distribution, the field will reach photoswitchable nanomagnets. Finally, photocontrol of the spin state of a unique molecule between two nanocontacts will offer new possibilities in the rising field of molecular spintronics.

Acknowledgment. We are grateful to our respective research institutions and to Magmanet, European network of excellence, for their financial support. We are also grateful for many fruitful discussions and help from our colleagues F. Baudelet, M. L. Boillot, A. Bousseksou, R. Clérac, P. Gütlich, K. Hashimoto, A. Hauser, J.-P. Itié, J. F. Létard, S. Ohkoshi, S. Ramasesha, H. Tokoro, F. Varret, and F. Villain. We are grateful to A. Bachschmidt, V. Escax, J.-M. Herrera, and J. Long for their valuable results on these systems. A special thanks is due to R. Lebris, ICMC Bordeaux, and R. Podgajny, Jagiellonian University, for their contribution to the field and their help in writing the manuscript.

(66) Hauser, A. *Coord. Chem. Rev.* **1991**, *111*, 275.